Title

Therapeutic efficacy of FASN inhibition in preclinical models of HCC

Journal

Hepatology, 76(4)

ISSN

0270-9139

Authors

Wang, Haichuan

Zhou, Yi

Xu, Hongwei

et al.

Publication Date

2022-10-01

DOI

10.1002/hep.32359

Peer reviewed

HHS Public Access

Author manuscript

Hepatology. Author manuscript; available in PMC 2023 October 01.

Published in final edited form as:

Hepatology. 2022 October ; 76(4): 951–966. doi:10.1002/hep.32359.

Therapeutic efficacy of FASN inhibition in preclinical models of HCC

Haichuan Wang[1,2], **Yi Zhou**[2,3], **Hongwei Xu**[1,2], **Xue Wang**[4], **Yi Zhang**[2,5], **Runze Shang**[2], **Marie O'Farrell**[6], **Stephanie Roessler**[7], **Carsten Sticht**[8], **Andreas Stahl**[4], **Matthias Evert**[9], **Diego F. Calvisi**[9,*], **Yong Zeng**[1,*], **Xin Chen**[2,*]

[1]Liver Transplantation Division, Department of Liver Surgery, West China Hospital, Sichuan University, Chengdu, China; Laboratory of Liver Surgery, West China Hospital, Sichuan University, Chengdu, Sichuan, China

[2]Department of Bioengineering and Therapeutic Sciences and Liver Center, University of California, San Francisco, California, USA

[3]Department of Infectious Diseases, The First Affiliated Hospital of Xi'an Jiaotong University, Xi'an, PR China

[4]Department of Nutritional Sciences and Toxicology, University of California Berkeley, Berkeley, California, USA

[5]Key Laboratory of Biorheological Science and Technology, Ministry of Education, College of Bioengineering, Chongqing University, Chongqing, China

[6]3-V Biosciences, Menlo Park, CA, USA

[7]Institute of Pathology, Heidelberg University, Heidelberg, Germany

[8]NGS Core Facility, Medical Faculty Mannheim, Heidelberg University, Heidelberg, Germany

[9]Institute of Pathology, University of Regensburg, Regensburg, Germany

Abstract

Background & Aims: Aberrant activation of fatty acid synthase (FASN) is a major metabolic event during the development of HCC. We evaluated the therapeutic efficacy of TVB3664, a novel FASN inhibitor, either alone or in combination, for HCC treatment.

Approach & Results: The therapeutic efficacy and the molecular pathways targeted by TVB3664, either alone or with tyrosine kinase inhibitors or the checkpoint inhibitor anti-PD-L1 antibody, were assessed in human HCC cell lines and multiple oncogene-driven HCC mouse

[*]**Corresponding authors:** Diego F. Calvisi, M.D., Institute of Pathology, University of Regensburg, Franz-Josef-Strauß-Allee 11, 93053 Regensburg, Germany. diego.calvisi@klinik.uni-regensburg.de; Yong Zeng, M.D, Ph.D., Department of Liver Surgery, Liver Transplantation Division, West China Hospital, Sichuan University, No. 37, Guo Xue Xiang, Chengdu, Sichuan 610041, China. zengyong@medmail.com.cn; Xin Chen, Ph.D., Department of Bioengineering and Therapeutic Sciences, University of California, San Francisco, CA 94143, USA. xin.chen@ucsf.edu.

Authors' Contributions: Haichuan Wang, Yi Zhou, Hongwei Xu, Xue Wang and Yi Zhang acquired experimental data. Marie O'Farrell provided administrative, technical, or material support. Haichuan Wang and Marie O'Farrell analyzed the data. Haichuan Wang drafted the manuscript. Andreas Stahl, Yong Zeng, Stephanie Roessler, Carsten Sticht, Diego F. Calvisi, and Xin Chen were involved in study design, drafting of the manuscript, study supervision, and obtaining funding.

Conflicts of interest: The authors have no conflicts of interest to disclose.

models. RNAseq was performed to elucidate the effects of TVB3664 on global gene expression and tumor metabolism. TVB3664 significantly ameliorated the fatty liver phenotype in the aged mice and AKT-induced hepatic steatosis. TVB3664 monotherapy showed moderate efficacy in NASH-related murine HCCs, induced by loss of PTEN and c-MET overexpression. TVB3664, in combination with cabozantinib, triggered tumor regression in this murine model but did not improve the responsiveness to immunotherapy. Global gene expression revealed that TVB3664 predominantly modulated metabolic processes, while TVB3664 synergized with cabozantinib to downregulate multiple cancer-related pathways, especially the AKT/mTOR pathway and cell proliferation genes. TVB3664 also improved the therapeutic efficacy of sorafenib and cabozantinib in the FASN-dependent c-MYC-driven HCC model. However, TVB3664 had no efficacy nor synergistic effects in FASN-independent murine HCC models.

Conclusions: This preclinical study suggests the limited efficacy of targeting FASN as monotherapy for HCC treatment. However, FASN inhibitors could be combined with other drugs for improved effectiveness. These combination therapies could be developed based on the driver oncogenes, supporting precision medicine approaches for HCC treatment.

Graphical Abstract

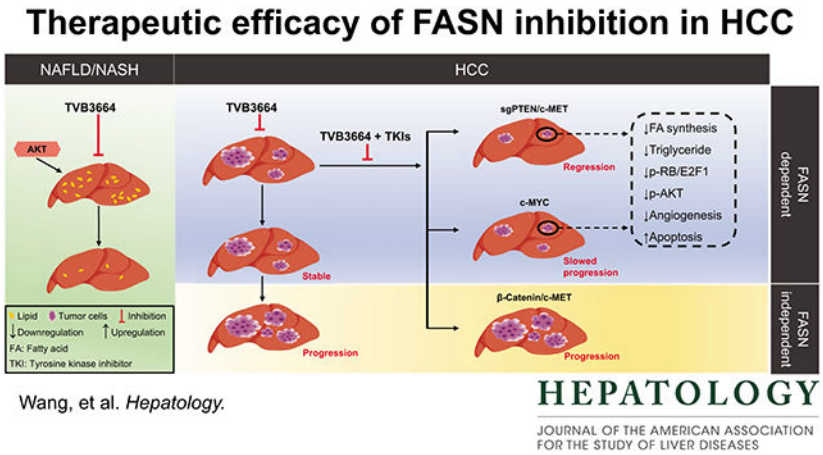

Keywords

Non-alcoholic steatohepatitis; Hepatocellular carcinoma; Fatty acid synthase; Cabozantinib; Combinational therapy

Introduction

Hepatocellular carcinoma (HCC) is the fourth most frequent cause of cancer-related deaths worldwide [(1)]. Metabolic disorders including diabetes, obesity, alcoholic fatty liver disease, and non-alcoholic fatty liver disease (NAFLD) are the common risk factors for HCC. HCC is frequently diagnosed at a late stage, and the curative approaches, such as surgical resection and liver transplantation, can only be applied to a small portion of patients. Systemic therapies, including receptor tyrosine kinase inhibitors (sorafenib, cabozantinib, etc.), immune-checkpoint inhibitors, especially anti-PDL1 combined with anti-VEGF-based therapies, have become the first- or second-line treatment options for advanced HCC [(2)].

However, most patients still progress under these therapies. Thus, additional studies are required to develop innovative and effective therapies against HCC.

Dysregulation of *de novo* lipogenesis has been linked to HCC molecular pathogenesis [3]. Aberrant lipid biosynthesis supplies the proliferating tumor cells with fatty acids required for energy production and membrane formation. *De novo* lipogenesis starts with ATP citrate lyase (ACLY) mediated conversion of citrate to acetyl-coenzyme A (CoA). CoA is then converted to malonyl-CoA by acetyl-CoA carboxylase (ACC) 1 and 2 and subsequently to fatty acids through the action of fatty acid synthase (FASN) [4]. As the major enzyme in lipogenesis, FASN expression depends tightly on the increased PI3K/AKT/mTOR signaling [5] and the activity of receptor tyrosine kinases (such as EGFR, c-Met, etc.) [6]. Importantly, *Fasn* deletion inhibits neoplastic conversion in several murine HCC models, such as HCCs induced by overexpression of AKT and c-MET (AKT/c-MET) [7], loss of PTEN and overexpression of c-MET (sgPTEN/c-MET) [8], or activation of c-MYC [9], thus supporting the crucial involvement of *de novo* lipogenesis in HCC development. On the other hand, functional studies suggest that FASN is dispensable for the growth of HCC induced by β-Catenin activation and c-MET overexpression (β-Catenin/c-MET) [10]. Altogether, these data indicate that *de novo* lipogenesis is required for hepatocarcinogenesis, depending on the oncogenes involved.

FASN inhibitors, such as C75, GSK2194069, and FAS31, have received substantial attention as potential pharmacological agents for cancer management [11]. Among them, TVB2640 is the most recent orally available FASN inhibitor [12]. In a phase 1 study in patients with advanced-stage solid malignant tumors (NCT02223247), responses to TVB-2640 have been detected across patients with *KRAS*-mutant lung, ovarian, and breast cancers [13]. Notably, TVB2640 significantly reduced liver fat content and improved biochemical, inflammatory, and fibrotic biomarkers in patients with non-alcoholic steatohepatitis (NCT03938246) [12]. However, in HCC, very few investigations assessed whether pharmacological inhibition of FASN can lead to tumor regression in preclinical models. Nevertheless, based on our genetic studies [8-10], we predict that FASN inhibitors likely have therapeutic potential against at least a subset of human HCCs. Importantly, because immunotherapy and tyrosine kinase inhibitors are still the therapies commonly used for advanced-stage HCC, anti-FASN drugs might be synergistic with these drugs for the treatment of HCC.

Here, we tested the anti-tumor effects of a novel FASN inhibitor, TVB3664, which has high potency against human and mouse FASN [14]. TVB3664 anti-neoplastic activity, either alone or combined with cabozantinib, sorafenib, or the anti-PD-L1 antibody, was evaluated in several clinically relevant oncogene-driven murine HCC models.

Materials and methods

Plasmids and reagents

The plasmids used in this study, including px330-Cas9-sgPTEN, pT3-EF1α-c-Met (human c-MET), pT3-EF1α-ΔN90-β-catenin (with N-terminal Myc-tag), pT3EF1α-c-Myc, pT3-EF1α-HA-myr-Akt (with N-terminal HA-tag), pT2CAGGS-NRasV12and pCMV/sleeping beauty transposase (SB), have been described previously in detail [15]. Cabozantinib (Cat#

C-8901) and sorafenib (Cat# S8502) were purchased from LC Laboratories (Woburn, Massachusetts, USA). Anti-mouse PD-L1 Ab was obtained from Genentech (South San Francisco, California, USA). TVB3664 was obtained from 3-V Biosciences (Menlo Park, California, USA).

Hydrodynamic tail vein injection

The wild-type *FVB/N* mice were obtained from Charles River Laboratories (Wilmington, MA, USA). The *Fasn*$^{flox/flox}$ conditional knockout mice in the C57BL/6J genetic background were described previously [16]. SB-mediated hydrodynamic tail vein injection was conducted as previously described [15]. Mice were housed, fed, and monitored according to protocols approved by the Committee for Animal Research at the University of California, San Francisco (San Francisco, CA, USA), protocol number AN185770. The abdominal girth and the signs of morbidity or discomfort were monitored for all mice.

Statistical analysis

GraphPad Prism V.9.2.0 (GraphPad Software Inc.) was used to analyze the data. Statistical analyses were conducted using Student's t-test, Mann-Whitney test, One-way ANOVA test, and Log-rank (Mantel-Cox) test analyses. Data are presented as mean ± SD. Values of $P < 0.05$ were considered statistically significant.

Additional information is available in Supporting Materials.

Results

TVB3664 improves fatty liver- and hepatic steatosis-related phenotypes

To investigate the role of TVB3664 on improving metabolic disorders in the liver, we first treated ~40 weeks old wild-type *FVB/N* mice with TVB3664, with the littermates treated with vehicle as control (Fig. S1A). The dosage responses of TVB3664 were determined previously, with 10mg/kg/day by oral gavage showing excellent bioavailability and pharmacokinetic properties in mice [14]. By the end of the three-week treatment, although no liver weight difference was found between the two groups (Fig. 1A), the levels of hepatic triglycerides, the main constituents of fatty acid, were significantly decreased in the TVB3664 treated mice (Fig. 1B). In addition, the TVB3664 treated group showed a consistent decrease in the levels of serum triglycerides (Fig. 1C). No other significant changes between the two groups as to the serum liver panel and lipid panels were noted (Fig. S1B). At the histological level, livers treated with TVB3664 appeared completely normal, with no signs of inflammation. The decreased lipid accumulation in the TVB3664 treated mice was also revealed by Oil-Red-O staining (Fig. 1D). Therefore, TVB3664 treatment improved fatty liver changes in the aged livers.

We have previously shown that FASN-mediated lipogenesis is required for AKT-driven hepatic steatosis [17]. Thus, we evaluated whether TVB3664 had similar effects as the genetic ablation of *Fasn* in this model. For this purpose, we injected *Fasn*$^{flox/flox}$ mice with HA-AKT and Cre recombinase (AKT/Cre) and additional *Fasn*$^{flox/flox}$ mice with HA-AKT and the pCMV empty vector (AKT/pCMV). One week post-injection (w.p.i), a subset of

AKT/pCMV mice were treated with TVB3664. In parallel, the rest of the AKT/pCMV mice and all AKT/Cre mice were treated with vehicle (Fig. 1E). Consistent with our previous report, AKT induced hepatic steatosis as seen in AKT/pCMV mice. In contrast, genetic ablation of *Fasn* completely prevented this phenotype, leading to decreased liver weight and lipid accumulation (Figs. 1F and 1G). Significantly, TVB3664 effectively suppressed AKT-induced hepatic steatosis (Figs. 1G, S2, and S3), as well as the hepatic triglyceride levels (Fig. S4), recapitulating the effect of *Fasn* deletion.

Furthermore, we detected a significant decrease of the main downstream effectors of *de novo* lipogenesis (*Scd1, Scd2, Elovl5, Elovl6*) in the TVB3664 treated livers at 5 w.p.i (Fig. 1H).

Altogether, our results prove that TVB3664 effectively inhibits fatty acid biosynthesis and improves fatty liver- and hepatic steatosis-related phenotypes in the mouse liver.

TVB3664 suppresses early-stage tumor growth in multiple murine HCC models

Previous genetic studies from our laboratory unraveled the requirement of FASN for HCC growth induced by multiple oncogenes, such as loss of PTEN (sgPTEN) and overexpression of c-MET (sgPTEN/c-MET) [8]. It is important to note that concurrent PTEN low expression [18] and MET overexpression[19] have been found in ~34% of human HCC patients (Fig. 2A), demonstrating poor survival outcomes [18] (Fig. 2B). Of note, as expression levels of PTEN reflect its biological function [20], we applied median values for *PTEN* mRNA levels as the cut-off. However, since the levels of its downstream targets mirror more accurately c-MET activation status, we used the expression levels of c-MET signature genes to define c-MET high levels.

The sgPTEN/c-MET tumor nodules start to emerge on the liver at ~5 w.p.i. Therefore, mice were treated with TVB3664 or vehicle starting at 6 w.p.i. At this time point, one group of mice was harvested as the pre-treatment control (Fig. 2C). Due to the diffused nature of our murine HCC models, the measurement of the number and size of tumor nodules could not accurately reflect tumor burden. Instead, using total liver weight as the tumor burden estimation, we found that TVB3664 treatment significantly reduced HCC growth compared to the vehicle control (Fig. 2D and Fig S5). Similar results were obtained when using the percentage of PTEN negative area as the tumor burden measurement (Fig. 2E and 2F). Moreover, cell proliferation and lipid accumulation were also significantly inhibited by the TVB3664 treatment, as measured by the percentage of Ki67 positive cells and Oil-Red-O staining, respectively (Fig. 2E and 2G). Of note, we did not find a significant difference between the pre-treatment group and the vehicle-treated group as to the percentage of Ki67 positive cells. This finding indicates that the tumor cells likely maintain high proliferative capacities starting from the pre-treatment time point until the end-point of observation (when the tissues in the vehicle group were harvested). In addition, TVB3664 treatment induced a significant decrease of hepatic triglyceride levels in the tumor tissues (Fig. 2H), supporting its role in inhibiting *de novo* lipogenesis. In contrast, the levels of total cholesterol (TC) and cholesteryl esters (CE) in the tumors were upregulated in the TVB3664 treated mouse HCCs compared to the vehicle-treated group (Fig. S6). The findings are consistent with our

previous report that cholesterol biosynthesis supports HCC growth in the absence of *de novo* lipogenesis [8].

Next, we investigate the underlying mechanisms of the TVB3664 anti-tumor effect by using Western blot analysis. Expression of metabolic-related molecules (Fig. S7A), major players of PI3K/AKT/mTOR signaling pathways (Fig. S7B), cell cycle and apoptosis proteins (Fig. S7C), and previously reported TVB3664 targets (Fig. S7D), were compared in normal livers from wild-type mice and pretreated-, vehicle-treated-, and TVB3664-treated- tumors (Fig. S8 and Fig. S9). The levels of cell cycle-related proteins (CCNB1, CCND1, CCNE, PCNA, and p-Rb) were moderately downregulated by TVB3664 (Fig. S7C and S9A), consistent with the reduction of the lesions' size and the reduction of proliferation (Fig. 2). As expected, FASN levels were not significantly changed among these groups (Fig. S8A), which is also consistent with the histological analysis (Fig. S10), because TVB3664 inhibits FASN activity without affecting FASN levels [14].

We then tested the anti-tumor efficacy of TVB3664 in another murine HCC model induced by AKT and NRAS activation (Fig. S11A). TVB3664 treatment started 2 w.p.i, when tumors emerge [21]. Again, TVB3664 significantly reduced HCC growth by inhibiting tumor cell proliferation, leading to increased survival of AKT/NRAS mice (Fig. S11).

Overall, the data indicate that TVB3664, administered at the early tumor stage, effectively inhibits the development of HCC induced by sgPTEN/c-MET and AKT/NRAS oncogenes.

TVB3664 synergizes with cabozantinib to inhibit HCC cell growth *in vitro*

As most HCCs are diagnosed at advanced stages, we sought to investigate TVB3664's efficacy when mice had a significant tumor burden. In the sgPTEN/c-MET model, liver weight over 3g was used as a moderate tumor burden. Intriguingly, in these late-stage tumor-bearing mice, TVB3664 demonstrated mild efficacy, and tumors continued to grow (data not shown). Therefore, we tested whether combinational therapy was able to improve therapeutic efficacy. Cabozantinib, which targets c-MET and VEGFR, was first tested as the potential synergistic agent. Human HCC cell lines with FASN and p-MET expression [22], including MHCC97H, HLE, and SNU449 cells, were treated with TVB3664 and cabozantinib, either alone or in combination. All three cell lines accumulated lipids upon oleate acid challenge, indicating the critical requirement of fatty acid for their growth (Fig. S12). Concomitant treatment of HCC cells with cabozantinib and TVB3664 resulted in more vigorous growth-inhibitory potency. We calculated the combination index (CI), and all CI values were lower than one in cabozantinib and TVB3664 treatment groups, implying a synergistic anti-tumor activity by the combination therapy (Fig. 3).

At the molecular level, cabozantinib inhibited p-MET expression. However, TVB3664 alone had a minor effect on the levels of examined proteins, including players of the RAS/MAPK and AKT/mTOR signaling pathways, cell cycle and apoptosis proteins, and main enzymes of metabolic processes. In contrast, the combinational treatment resulted in a pronounced inhibition of p-AKT^{Thr308}, p-AKT^{Ser473}, p-RPS6, SCD1, and cell cycle-related proteins (CCND1, CCNE, and p-Rb) expression and upregulation of cell apoptosis proteins (cleaved

caspase-3 and cleaved caspase-7). Furthermore, levels of prominent metabolic players remained generally unchanged (Fig. S13).

In summary, the present results indicate that TVB3664 synergizes with cabozantinib to constrain HCC growth *in vitro*.

Combined TVB3664/cabozantinib leads to sgPTEN/c-MET HCC regression

Next, we investigated the synergistic effects *in vivo* using the late-stage sgPTEN/c-MET murine HCC model. The treatment started at 12 w.p.i., when moderate tumor burden is evident (liver weight ~3g). Mice were orally fed TVB3664 and cabozantinib, either alone or in combination. One additional group was treated with vehicle as control, and another arm of mice was harvested when treatment started as the 'pre-treatment' control (Fig. 4A). Using total liver weight to measure tumor burden, we found that monotherapy induced moderate (cabozantinib) or very mild (TVB3664) anti-tumor effects. However, tumor burden was still higher than that of the pre-treatment cohort, implying slower, yet still progressive, tumor growth. In contrast, the combination therapy showed decreased tumor burden than the pre-treatment mice (Fig. 4B and Fig. S14), indicating tumor regression.

At the cellular level, the percentages of PTEN negative areas and Ki67 positive cells in the tumors were significantly lower in the combinational groups compared to vehicle-treated- or single reagent-treated groups (Fig. 4C-E). Expression of FASN and ACC inside the tumor nodules showed no significant changes (Fig. S15). As expected, tumor angiogenesis, measured by the percentage of CD34 immunoreactivity positive areas, was significantly reduced in the cabozantinib and the combinational treated tumors (Fig. 4F and Fig. S16). In addition, we found a significant decrease in lipid accumulation in the tumor nodules treated with TVB3664 (both TVB3664 and combinational groups; Fig. 4C).

Serum levels of hepatic enzymes showed no significant change in the drug-treated groups compared to the vehicle-treated group (Fig. S17A). Interestingly, we noted severe hyperlipidemia in the sgPTEN/c-MET tumor-bearing mice, while this condition was ameliorated in the combinational treated mice, consistent with the changes revealed by serum lipid panels (Fig. S17B).

In summary, TVB3664 synergizes with cabozantinib to regulate fatty acid metabolism and cell cycle, leading to the regression of sgPTEN/c-MET mouse tumors.

Combined TVB3664/anti-PD-L1 treatment does not increase therapeutic efficacy in the sgPTEN/c-MET HCCs

Previous studies have shown that NASH–HCCs are less responsive to immunotherapy due to aberrant T cell activation [23]. Thus, we investigated whether TVB3664 could modulate the immune environment to tailor combinational immunotherapies. The F4/80+ macrophage cells and CD45+, CD8+ T cells were first revealed by immunohistochemical staining in pretreated, vehicle-treated, and TVB3664-treated sgPTEN/c-MET tumors. However, no significant difference was found (Fig. S18).

Next, we tested whether combining TVB3664 and anti-PD-L1 antibody administration can increase growth inhibition in the NASH-related sgPTEN/c-MET HCC lesions. Thus, mice were treated with TVB3664 and anti-PD-L1, either alone or combined (Fig. S19A). We found that, overall, PD-L1 had no efficacy against sgPTEN/c-MET mouse HCC, and TVB3664 did not synergize to improve the therapeutic effectiveness (Fig. S19).

Altogether, these findings suggest that TVB3664 does not modulate the immune environment in NASH-related tumors. Combined TVB3664 and anti-PD-L1 treatment has limited therapeutic efficacy in the murine models tested.

Global gene expression profiling of the TVB3664 and/or cabozantinib treated sgPTEN/c-MET HCC

To comprehensively investigate the functional mechanisms underlying the synergistic effects, we performed RNAseq analysis of the wild-type normal livers and vehicle-, cabozantinib-, TVB3664- and combinational- treated late-stage sgPTEN/c-MET mouse tumors (GSE189529). The differentially expressed genes (DEG) in each group were subject to the multidimensional scaling analysis. Genetic dissimilarities between the vehicle and combinational groups were evident. The cabozantinib and the TVB3664 groups stood between the vehicle and combinational groups (Fig. 5A). Next, we analyzed DEG in each group considering all genes (Fig. S20). Similar to the multidimensional scaling analysis, the top 50 DEG showed a clear separation between the treatment and vehicle groups (Fig. S20A). Analysis of the canonical pathways revealed common and distinct signaling cascades, with senescence being enriched in the cabozantinib and combination groups (Fig. S20B). Furthermore, several upstream regulators were predicted to be inhibited. Among them, *VEGF* and *HGF* were suggested to be preferentially suppressed in the cabozantinib and combinational treament group, confirming the results obtained in late stage tumors (Fig. S20C-E). For downregulated genes. TVB3664 treatment decreased fewer genes (N=141) than cabozantinib treatment group (N=349). As expected, the combinational therapy led to the most downregulated genes (N=1082; Fig. 5B). Consistently, the number of upregulated genes in the TVB3664 (N=482) and cabozantinib (N=542) group was lower than in the combinational treatment group (N=1337; Fig. S21A). Overall, the gene expression analysis suggest that TVB3664 alone had a limited effect on the overall gene expression program, while it was synergistic when combined with cabozantinib.

The KEGG analysis of the downregulated genes suggested that TVB3664 mainly affected the metabolic pathways (Fig. 5C and Supporting Table S1), whereas cabozantinib primarily inhibited key cancer-related pathways, such as the RAS/MAPK pathway and cellular senescence (Fig. 5D and Supporting Table S2). Interestingly, in addition to the ones noted in the cabozantinib group, the DEG in the combinational treatment group also clustered in the PI3K-AKT pathway, p53 pathway, and cell cycle cascades (Fig. 5E and Supporting Table S3). Also, the prominent cell cycle-related genes were significantly decreased in the combinational treatment group (Fig. S22). The significant downregulation of p-AKT^{Thr308} and cell cycle-related proteins (CCND1, PCNA, and p-Rb) in the combinational group was further confirmed by Western blot analysis (Fig. 5F). In addition, the KEGG analysis revealed that the treatments induced the upregulation of genes in metabolism-related

pathways. Furthermore, TVB3664 affected the AMPK and Hippo pathways, cabozantinib shaped the HIF-1 signaling, and the combinational therapy altered the PPAR molecular cascade (Fig. S21B-D).

In summary, the present results indicate that TVB3664 monotherapy has a limited effect on global gene expression. However, when combined with cabozantinib, TVB3664 demonstrates a synergistic anti-tumor effect via inhibiting the PI3K/AKT pathway and cell cycle progression.

TVB3664 synergizes with tyrosine kinase inhibitors to slow c-MYC tumor progression

Triggered by the exciting outcomes of the combinational treatment, we aimed to test whether it is actionable in other oncogene-driven HCC models. c-MYC amplification/activation occurs in ~20-30% human HCC samples, and *Fasn* genetic depletion is detrimental for c-MYC HCC growth [(9)]. Therefore, we speculated that TVB3664 based combinational approaches might also effectively treat c-MYC induced HCC. We have previously shown that cabozantinib monotherapy has limited efficacy against c-MYC tumors [(22)]. In addition, our preliminary data showed that sorafenib, one of the major targeted therapeutic drugs for advanced HCC, was also ineffective. Thus, we tested whether these approved agents for HCC treatment have a synergistic anti-tumor effect with TVB3664 in c-MYC tumors.

c-MYC tumors were treated with TVB3664, cabozantinib, and sorafenib, either alone or in combination at 5.5w.p.i. At this time point, all mice had moderate HCC burden with liver weight around ~3g. One additional group was treated with vehicle as control, and another arm of mice was harvested when treatment started as the 'pre-treatment' control (Fig. 6A). As a result, c-MYC tumors still progressed on cabozantinib or TVB3664 monotherapy. Both cabozantinib/TVB3664 and sorafenib/TVB3664 combinational treatments led to significant tumor growth inhibition compared to monotherapy. However, in comparison to the pre-treatment cohort, tumor burden was still higher, suggesting that the combination therapies significantly slowed HCC progression. (Fig. 6B and Fig. S23). Next, we determined the c-MYC (+) area percentages, as another measurement for tumor burden, within the tumor tissues using the anti-c-MYC immunohistochemical staining [(24)]. Notably, both the cabozantinib/TVB3664 and sorafenib/TVB3664 treatments decreased the c-MYC (+) neoplastic areas, and sorafenib/TVB3664 was more effective (Fig. 6C, Fig. S24, and S25).

At the cellular level, all the treatments effectively inhibited tumor cell proliferation, with the sorafenib/TVB3664 combinational group showing the most significant decrease (Fig. 6D and Fig. S26). Intriguingly, the cabozantinib treated c-MYC tumor, either monotherapy or combinational therapy, demonstrated more pronounced cellular apoptosis as revealed by remarkable cleaved caspase-3 immunoreactivity (Fig. 6E and Fig. S27). Additionally, cabozantinib, sorafenib, and TVB3664, either alone or in combination, significantly hampered tumor angiogenesis, as assessed by CD34 staining (Fig. 6F and Fig. S28).

Interestingly, consistent with the findings in the sgPTEN/c-MET model, TVB3664 treatment also led to a significant decrease of hepatic triglycerides levels in the c-MYC tumor tissues (Fig. S29A). In addition, the levels of TC and CE in the tumors were upregulated, while TC

and free cholesterols (FC) in the surrounding tissues were downregulated in the TVB3664 treated groups compared to the vehicle-treated group (Fig. S29B, C). However, the levels of the main metabolic-related proteins and the AKT/mTOR and MAPK signaling kinases were not consistently affected by TVB3664 treatment (Fig. S30A and S30B). Instead, the expression of p-Rb was consistently decreased in the TVB3664 treated tumors (Fig. S30C). Moreover, TVB3664 in combination with cabozantinib or sorafenib resulted in a more significant decrease in p-AKT^{Ser473} and cell cycle-related protein CCND1 expression (Fig. S31).

Altogether, TVB3664 synergizes with tyrosine kinase inhibitors to inhibit c-MYC induced HCCs, leading to slowed tumor progression. The results envisage the potential to employ TVB3664 based combination therapy to FASN dependent HCC subtypes.

TVB3664 is unable to improve cabozantinib anti-tumor effects in FASN-independent models

Mutations of *CTNNB1* are one of the most frequent genetic events in human HCCs [18]. Our previous investigation demonstrated that ablation of *Fasn* does not affect murine HCC induced by CTNNB1 gain of function mutation and c-MET overexpression (referred to as β-CateninΔ90/c-MET HCC) [10]. To determine the specificity of TVB3664 for effectively treating FASN-dependent HCC, we treated β-CateninΔ90/c-MET tumor-bearing mice with TVB3664, either alone or in combination with cabozantinib, starting at 6w.p.i. One additional group was treated with vehicle as control, and another arm of mice was harvested when treatment began as the 'pre-treatment' control (Fig. 7A). Using liver weight as tumor burden measurement, cabozantinib monotherapy led to stable disease in β-CateninΔ90/c-MET mice, consistent with our previous report [22]. However, TVB3664 treatment had no efficacy. Moreover, TVB3664/cabozantinib combinational treatment showed no difference with the cabozantinib monotherapy group (Fig. 7B). Taking advantage of Myc-tagged-β-CateninΔ90 staining, we quantified the percentage of Myc-tag positive area as another method for tumor burden measurement, and consistent results were obtained (Figs. 7C and 7D). At the cellular level, tumor cell proliferation, indicated by the percentage of Ki67 positive cells, was decreased in the cabozantinib and cabozantinib/TVB3664 treated tumors (Figs. 7C and 7E). Additionally, no consistent changes in the major players of RAS/MAPK and AKT/mTOR signaling pathways, cell cycle and apoptosis proteins, and main metabolic enzymes were observed in the TVB3664 treated β-CateninΔ90/c-MET tumors (Fig. S32).

Taken together, in a FASN independent HCC model, TVB3664 treatment did not demonstrate any efficacy, nor did it potentiate the therapeutic efficacy in combination therapy. Thus, TVB3664 should only be applied to FASN-dependent HCC models.

Discussion

With the increasing prevalence of NAFLD/NASH and related HCC development [25], preventive and curative strategies are in great demand. FASN and its mediated *de novo* lipogenic metabolic cascades play a pivotal pathological role during these processes. Potent and selective FASN small-molecule inhibitors (TVB2640, TVB3166, TVB3693, and TVB3664) have recently been described [14, 26, 27]. Compared with the early generation

FASN inhibitors, such as cerulenin, orlistat, and C75, the TVB compounds exhibit significantly improved potency and selectivity. In addition, the TVB drugs are typically well-tolerated in animals, according to preclinical studies. TVB2640 is currently tested in phase II clinical trials in combination with other therapeutic agents. Its analogs, TVB3166 and TVB3664, have shown anticancer activity in lung, prostate, ovarian, and colorectal cancer models *in vitro* and *in vivo* [14, 27, 28]. Our present study shows that TVB3664 effectively inhibits *de novo* lipogenesis and improves NAFLD/NASH-related effects in old mice and AKT overexpressing livers. Studies on the Western diet-induced murine NASH models also showed that TVB3664 treatment was associated with a dose-dependent reduction in liver histology severity score (unpublished data), suggesting TVB3664 as a potent drug for NAFLD/NASH treatment. In addition, we demonstrated that TVB3664 synergized with cabozantinib to induce NASH-related sgPTEN/c-MET murine HCC regression. Of note, in addition to the oncogene-driven HCC models, several preliminary studies also reported that TVB3664 reduces fat content, inflammation, and fibrosis and inhibits tumorigenesis in the NASH murine model induced by high fat-cholesterol Western diet and glucose-fructose sugar water in combination with CCl_4 injection [29]. In perspective, it would also be beneficial to test the effects of TVB3664 combinational therapy in these chemically-induced tumors to provide reliable preclinical support for testing TVB3664 (or TVB2640) in clinical trials.

Mechanistically, the sequencing data demonstrated that TVB3664 monotherapy mainly affected genes related to metabolic processes. Interestingly, we also found that key genes belonging to the RB/E2F1 pathway, such as *Cdc6, E2f1, Mcm4*, and *Skp2,* were also downregulated by TVB3664. Furthermore, consistent results were found in the AKT, sgPTEN/c-MET, and c-MYC models (Fig. S33). Considering that E2F1 has been recently shown to mediate sustained lipogenesis and contribute to hepatic steatosis [30], the present findings add on the underlying mechanisms of TVB3664 on suppressing fatty acid biosynthesis. However, the overall anti-tumor effect of TVB3664 monotherapy is yet impotent, especially for the intermediate to late-stage HCCs. Hence, combinational therapies, such as TVB3664 in combination with tyrosine kinase inhibitors, would be more vigorous in this context. Importantly, TVB3664 synergized with cabozantinib (or sorafenib) to additionally suppress the AKT/mTOR signaling and cell cycle genes. Of note, although the applications of AKT and/or mTOR inhibitors showed an efficient tumor growth inhibition capacity *in vitro* and *in vivo*, the clinical trials so far conducted failed to reach compelling outcomes [31], in part due to the dose limiting toxicities of these inhibitors as AKT/mTOR pathway has key roles in regulating various metabolic pathways and immunity [32]. Therefore, FASN inhibitors holds the promise as a substitute where AKT/mTOR inhibitors are in need. Importantly, the *in vitro* studies using C75, another FASN inhibitor, showed that C75 and cabozantinib concomitant treatment resulted in increased growth inhibition in human HCC cell lines (Fig. S34). Overall, the results highlight the importance of targeting fatty acid synthetase to treat HCCs.

It is worth mentioning that the main function of TVB3664 is to inhibit the keto-reductase enzymatic function of fatty acid synthase [27]. At the transcription level, TVB3664 suppressed the expression of transcriptional regulating genes of *de novo* lipogenesis sterol regulatory element-binding protein 1c (SREBP1c, encoded by *Srebf1*) and liver X receptors

alpha (encoded by *Nr1h3*). However, no other significant difference in the genes related to *de novo* lipogenesis was found (Fig. S35). Glycolysis is also a critical source for tumor cell proliferation. The pyruvate produced by glycolysis is an essential intermediary for converting carbohydrates into fatty acids and cholesterol. The expression of genes encoding glycolytic enzymes in the sgPTEN/c-MET HCC tumors was not significantly affected by TVB3664 (Fig. S36). Consistently, the protein expressions of these enzymes were not affected by TVB3664 either among the sgPTEN/c-MET, c-MYC or β-CateninΔ90/c-MET tumor lesions (Figs. S7, S30, and S32).

In the present study, TVB3664, in combination with PD-L1 treatment, was unable to inhibit tumor growth, which might be due to the immunosuppressive characteristic of HCC. It has been reported that fatty acid oxidation drives the suppressor function of regulatory T cells [(33)]. However, TVB3664 administration did not affect the expression of genes controlling the β-oxidation cycle or regulatory T cells specific marker *Foxp3* (Fig. S37), at least based on the RNAseq study. Further investigations at the single-cell resolution might provide more in-depth information about tumor immune environment adaptiveness upon fatty acid metabolism changes.

Among the critical questions that remain to be addressed for the clinical practice is how the HCC patients can be selected for anti-FASN treatments. It is clear from the HCC TCGA analysis [(18)] and other genomic studies that human HCCs are highly heterogeneous. Notably, HCCs driven by distinct oncogenes are either dependent or independent from *de novo* lipogenesis to grow [(3)]. Using $Fasn^{flox/flox}$ conditional *KO* mice, we have previously shown that sgPTEN/c-MET and c-MYC mouse HCCs are addicted to FASN, while FASN is dispensable for β-CateninΔ90/c-MET induced hepatocarcinogenesis [(8-10)]. Consistently, our present study indicates that TVB3664 (in combination with cabozantinib) effectively suppresses the growth of FASN-dependent sgPTEN/c-MET and c-MYC murine HCCs. In contrast, it has no anti-tumor efficacy in FASN-independent β-CateninΔ90/c-MET hepatocarcinogenesis (Fig. S38). It has been demonstrated that β-catenin-induced HCCs use PPARα mediated fatty acid oxidation as an energy source while exhibit lower esterification rates and reduced lipogenesis, which is rerouted towards phospholipid synthesis [(34)]. It is possible that β-CateninΔ90/c-MET tumor cells efficiently take advantage of exogenous fatty acid uptake for growth and proliferation. Therefore, the FASN inhibitor TVB3664 marginally improves the anti-tumor activity of cabozantinib in the β-CateninΔ90/c-MET mouse HCCs. Thus, the combination of fatty acid transporter inhibitors, such as grassofermata [(35)] and lipofermata [(36)], with TKIs can be investigated in this subtype of HCC. Clearly, from the perspective of precision medicine, reliable biomarkers able to uncover the patients who would presumably benefit from this therapeutic strategy should be identified. Thus, future studies are required to evaluate the therapeutic potential of anti-FASN drugs for the treatment of HCC, especially in those patients whose tumors show elevated activation of the AKT/mTOR/lipogenesis cascade.

Supplementary Material

Refer to Web version on PubMed Central for supplementary material.

Acknowledgment:

We thank George Kemble at 3-V Biosciences (Menlo Park, CA, USA) and Bruce Wang at the University of California, San Francisco (San Francisco, CA, USA) for scientific discussions. We also thank the Parnassus Center for Advanced Technologies at the University of California, San Francisco, for technical supports.

Financial support:

This study was supported by NIH grants R01CA204586, R01CA239251, R01CA250227 and R03CA288375 to XC, P30DK026743 for UCSF Liver Center; National Natural Science Foundation (82002967) to HW. SR was supported by funds from German Cancer Aid (Deutsche Krebshilfe, project no. 70113922) and European Union's Horizon 2020 research and innovation programme under Eurostars (grant E! 113707, LiverQR).

Data availability statement:

The RNAseq data for this study were deposited in the Gene Expression Omnibus database (GSE189529). Other data that support the findings of this study are included within the article and its supplementary materials.

List of Abbreviations

FASN	fatty acid synthase
HCC	hepatocellular carcinoma
NAFLD	non-alcoholic fatty liver disease
NASH	non-alcoholic steatohepatitis
ACLY	ATP citrate lyase
ACC	acetyl-CoA carboxylase
TC	total cholesterol
CE	cholesteryl ester
CI	combination index
DEG	differential expression genes
KEGG	Kyoto Encyclopedia of Genes and Genomes

References

1. Sung H, Ferlay J, Siegel RL, Laversanne M, Soerjomataram I, Jemal A, et al. Global cancer statistics 2020: Globocan estimates of incidence and mortality worldwide for 36 cancers in 185 countries. CA Cancer J Clin 2021;71:209–249. [PubMed: 33538338]
2. Gordan JD, Kennedy EB, Abou-Alfa GK, Beg MS, Brower ST, Gade TP, et al. Systemic therapy for advanced hepatocellular carcinoma: Asco guideline. J Clin Oncol 2020;38:4317–4345. [PubMed: 33197225]
3. Zhou Y, Tao J, Calvisi DF, Chen X. Role of lipogenesis rewiring in hepatocellular carcinoma. Semin Liver Dis.
4. Satriano L, Lewinska M, Rodrigues PM, Banales JM, Andersen JB. Metabolic rearrangements in primary liver cancers: Cause and consequences. Nat Rev Gastroenterol Hepatol 2019;16:748–766. [PubMed: 31666728]

5. Matter MS, Decaens T, Andersen JB, Thorgeirsson SS. Targeting the mTOR pathway in hepatocellular carcinoma: Current state and future trends. J Hepatol 2014;60:855–865. [PubMed: 24308993]
6. Giordano S, Columbano A. Met as a therapeutic target in HCC: Facts and hopes. J Hepatol 2014;60:442–452. [PubMed: 24045150]
7. Hu J, Che L, Li L, Pilo MG, Cigliano A, Ribback S, et al. Co-activation of AKT and c-MET triggers rapid hepatocellular carcinoma development via the mtorc1/fasn pathway in mice. Sci Rep 2016;6:20484. [PubMed: 26857837]
8. Che L, Chi W, Qiao Y, Zhang J, Song X, Liu Y, et al. Cholesterol biosynthesis supports the growth of hepatocarcinoma lesions depleted of fatty acid synthase in mice and humans. Gut 2020;69:177. [PubMed: 30954949]
9. Jia J, Che L, Cigliano A, Wang X, Peitta G, Tao J, et al. Pivotal role of fatty acid synthase in c-MYC driven hepatocarcinogenesis. Int J Mol Sci 2020;21.
10. Che L, Pilo MG, Cigliano A, Latte G, Simile MM, Ribback S, et al. Oncogene dependent requirement of fatty acid synthase in hepatocellular carcinoma. Cell Cycle 2017;16:499–507. [PubMed: 28118080]
11. Röhrig F, Schulze A. The multifaceted roles of fatty acid synthesis in cancer. Nature Reviews Cancer 2016;16:732–749. [PubMed: 27658529]
12. Loomba R, Mohseni R, Lucas KJ, Gutierrez JA, Perry RG, Trotter JF, et al. TVB-2640 (FASN inhibitor) for the treatment of nonalcoholic steatohepatitis: Fascinate-1, a randomized, placebo-controlled phase 2a trial. Gastroenterology 2021;161:1475–1486. [PubMed: 34310978]
13. Falchook G, Infante J, Arkenau H-T, Patel MR, Dean E, Borazanci E, et al. First-in-human study of the safety, pharmacokinetics, and pharmacodynamics of first-in-class fatty acid synthase inhibitor TVB-2640 alone and with a taxane in advanced tumors. EClinicalMedicine 2021;34.
14. Heuer TS, Ventura R, Mordec K, Lai J, Fridlib M, Buckley D, et al. Fasn inhibition and taxane treatment combine to enhance anti-tumor efficacy in diverse xenograft tumor models through disruption of tubulin palmitoylation and microtubule organization and fasn inhibition-mediated effects on oncogenic signaling and gene expression. EBioMedicine 2017;16:51–62. [PubMed: 28159572]
15. Chen X, Calvisi DF. Hydrodynamic transfection for generation of novel mouse models for liver cancer research. Am J Pathol 2014;184:912–923. [PubMed: 24480331]
16. Chakravarthy MV, Zhu Y, López M, Yin L, Wozniak DF, Coleman T, et al. Brain fatty acid synthase activates pparα to maintain energy homeostasis. J Clin Invest 2007;117:2539–2552. [PubMed: 17694178]
17. Li L, Pilo GM, Li X, Cigliano A, Latte G, Che L, et al. Inactivation of fatty acid synthase impairs hepatocarcinogenesis driven by akt in mice and humans. J Hepatol 2016;64:333–341. [PubMed: 26476289]
18. Ally A, Balasundaram M, Carlsen R, Chuah E, Clarke A, Dhalla N, et al. Comprehensive and integrative genomic characterization of hepatocellular carcinoma. Cell 2017;169:1327–1341.e1323. [PubMed: 28622513]
19. Qiao Y, Wang J, Karagoz E, Liang B, Song X, Shang R, et al. Axis inhibition protein 1 (Axin1) deletion–induced hepatocarcinogenesis requires intact β-Catenin but not NOTCH cascade in mice. Hepatology 2019;70:2003–2017. [PubMed: 30737831]
20. Villanueva A, Chiang DY, Newell P, Peix J, Thung S, Alsinet C, et al. Pivotal role of mTOR signaling in hepatocellular carcinoma. Gastroenterology 2008;135:1972–1983.e1911. [PubMed: 18929564]
21. Ho C, Wang C, Mattu S, Destefanis G, Ladu S, Delogu S, et al. Akt (v-akt murine thymoma viral oncogene homolog 1) and n-Ras (neuroblastoma ras viral oncogene homolog) coactivation in the mouse liver promotes rapid carcinogenesis by way of mTOR (mammalian target of rapamycin complex 1), FOXM1 (forkhead box m1)/SKP2, and c-MYC pathways. Hepatology 2012;55:833–845. [PubMed: 21993994]
22. Shang R, Song X, Wang P, Zhou Y, Lu X, Wang J, et al. Cabozantinib-based combination therapy for the treatment of hepatocellular carcinoma. Gut 2021;70:1746. [PubMed: 33144318]

23. Pfister D, Núñez NG, Pinyol R, Govaere O, Pinter M, Szydlowska M, et al. NASH limits anti-tumour surveillance in immunotherapy-treated HCC. Nature 2021;592:450–456. [PubMed: 33762733]
24. Gill T, Wang H, Bandaru R, Lawlor M, Lu C, Nieman LT, et al. Selective targeting of MYC mRNA by stabilized antisense oligonucleotides. Oncogene 2021.
25. Younossi Z, Anstee QM, Marietti M, Hardy T, Henry L, Eslam M, et al. Global burden of NAFLD and NASH: Trends, predictions, risk factors and prevention. Nat Rev Gastroenterol Hepatol 2018;15:11–20. [PubMed: 28930295]
26. Buckley D, Duke G, Heuer TS, O'Farrell M, Wagman AS, McCulloch W, et al. Fatty acid synthase – modern tumor cell biology insights into a classical oncology target. Pharmacol Ther 2017;177:23–31. [PubMed: 28202364]
27. Ventura R, Mordec K, Waszczuk J, Wang Z, Lai J, Fridlib M, et al. Inhibition of de novo palmitate synthesis by fatty acid synthase induces apoptosis in tumor cells by remodeling cell membranes, inhibiting signaling pathways, and reprogramming gene expression. EBioMedicine 2015;2:808–824. [PubMed: 26425687]
28. Zaytseva YY, Rychahou PG, Le A-T, Scott TL, Flight RM, Kim JT, et al. Preclinical evaluation of novel fatty acid synthase inhibitors in primary colorectal cancer cells and a patient-derived xenograft model of colorectal cancer. Oncotarget 2018;9.
29. Bhattacharya D, Duke G, Allen B, Ybanez MCD, Kemble G, Friedman SL. The FASN inhibitor, TVB3664, ameliorates nash in a murine model [abstract]. Hepatology 2018;68:184–1353.
30. Denechaud P-D, Lopez-Mejia IC, Giralt A, Lai Q, Blanchet E, Delacuisine B, et al. E2F1 mediates sustained lipogenesis and contributes to hepatic steatosis. J Clin Invest 2016;126:137–150. [PubMed: 26619117]
31. Wang H, Chen X, Calvisi DF. Hepatocellular carcinoma (HCC): The most promising therapeutic targets in the preclinical arena based on tumor biology characteristics. Expert Opin Ther Targets 2021;25:645–658. [PubMed: 34477018]
32. Zhang Y, Yan H, Xu Z, Yang B, Luo P, He Q. Molecular basis for class side effects associated with PI3K/AKT/mTOR pathway inhibitors. Expert Opin Drug Metab Toxicol 2019;15:767–774. [PubMed: 31478386]
33. Gualdoni GA, Mayer KA, Göschl L, Boucheron N, Ellmeier W, Zlabinger GJ. The amp analog aicar modulates the Treg/Th17 axis through enhancement of fatty acid oxidation. FASEB J 2016;30:3800–3809. [PubMed: 27492924]
34. Senni N, Savall M, Cabrerizo Granados D, Alves-Guerra M-C, Sartor C, Lagoutte I, et al. β-Catenin-activated hepatocellular carcinomas are addicted to fatty acids. Gut 2019;68:322. [PubMed: 29650531]
35. Saini N, Black PN, Montefusco D, DiRusso CC. Fatty acid transport protein-2 inhibitor Grassofermata/CB5 protects cells against lipid accumulation and toxicity. Biochem Biophys Res Commun 2015;465:534–541. [PubMed: 26284975]
36. Zhang M, Di Martino JS, Bowman RL, Campbell NR, Baksh SC, Simon-Vermot T, et al. Adipocyte-derived lipids mediate melanoma progression via FATP proteins. Cancer Discov 2018;8:1006. [PubMed: 29903879]

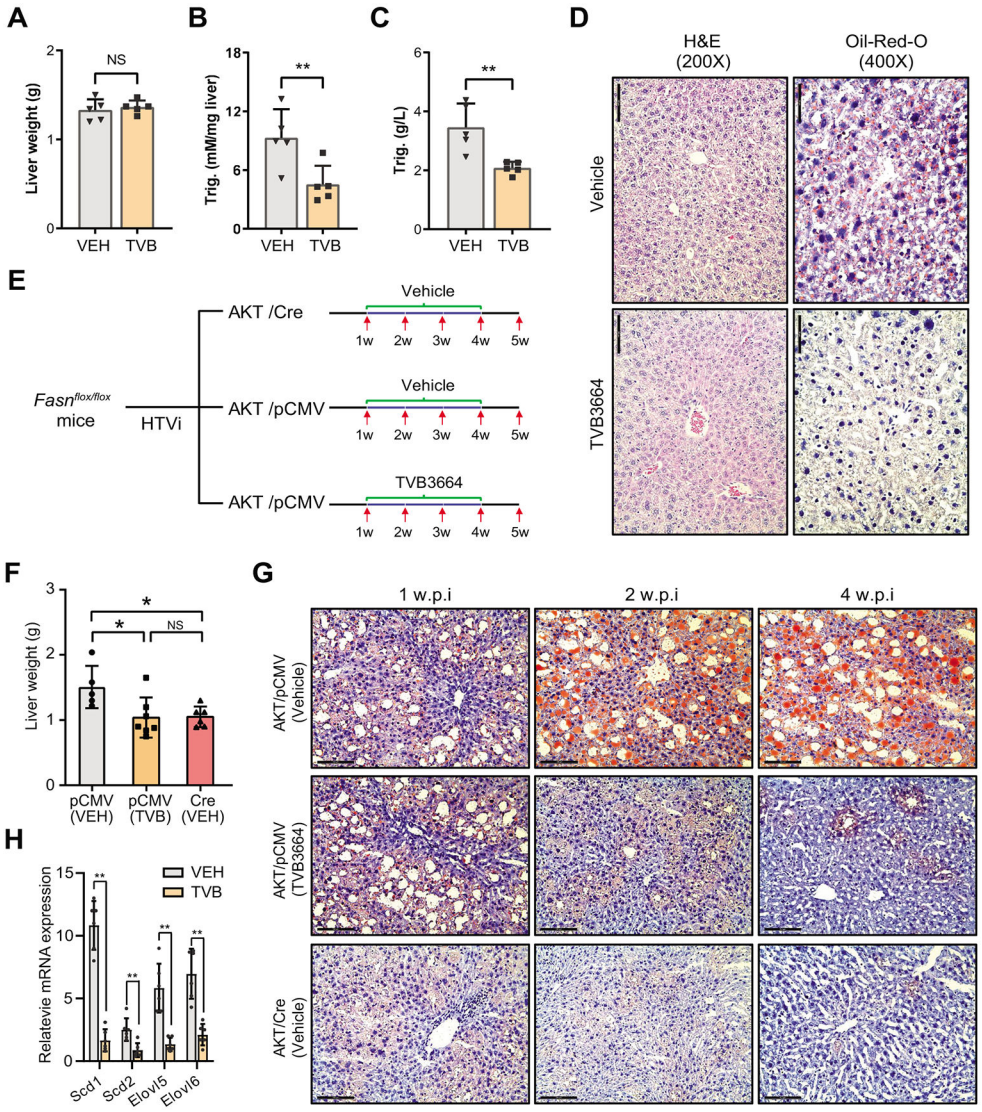

Fig. 1. TVB3664 restrains lipid accumulation in the liver.

(A) Liver weight of the mice treated with vehicle (VEH) and TVB3664 (TVB) at the time of sacrifice. The ~40 weeks old *FVB/N* mice were treated with TVB3664 (N=5, 10mg/kg/d) or vehicle (N=5) through daily oral gavage for 3 weeks and then sacrificed for the following analysis. **(B, C)** Hepatic triglyceride (B) and serum triglyceride (C) levels. **(D)** Representative images of H&E and Oil-Red-O stainings of vehicle or TVB3664 treated aged *FVB/N* mice. Scale bars: 100μm for H&E, 50μm for Oil-Red-O. **(E)** Study design. *Fasn*$^{flox/flox}$ mice were hydrodynamically injected with HA-AKT/pCMV and HA-AKT/Cre. As indicated, mice were treated with Vehicle or TVB3664, starting from 1 week after injection. Mice livers were harvested at 1, 2, 3, 4, 5-weeks after injection. **(F)** Liver weight at 5 weeks after injection. **(G)** Representative images of Oil-Red-O stainings. Scale bars: 100μm. **(H)** Expression of FASN downstream targets. Samples collected from the end-point were used for this analysis. (A, B, C, H) Mean ± SD; Mann-Whitney test. (F) Mean ± SD; One-way ANOVA test. *, P<0.05, **, P<0.01, NS, no significance.

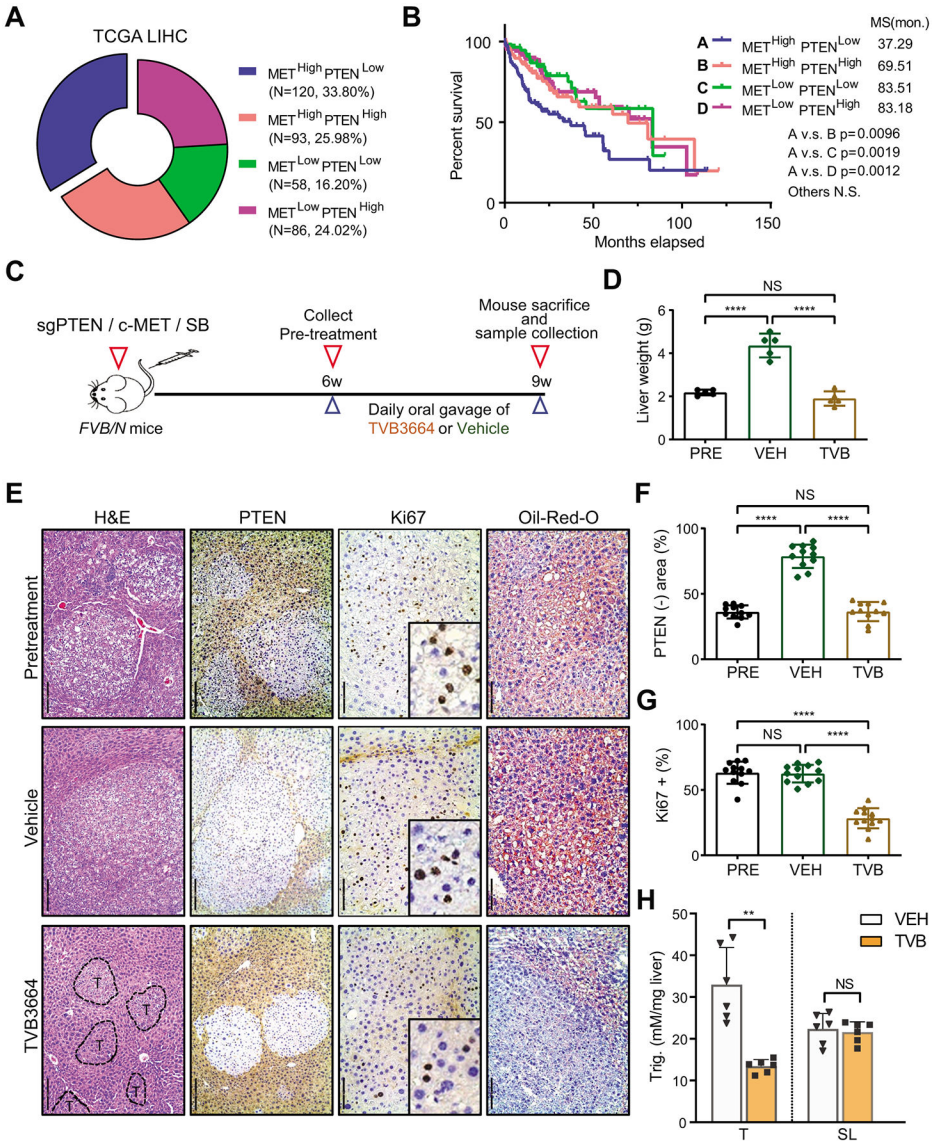

Fig. 2. TVB3664 treatment inhibits the growth of sgPTEN/c-MET mouse HCCs.

(A) Analysis of the MET signature and PTEN expression levels in human HCC samples based on the TCGA LIHC dataset. **(B)** $MET^{High}/PTEN^{Low}$ HCC (N = 120) showed a poor survival outcome when compared with other subgroups in human HCC patients. The median survival time (MS) of each group is shown as indicated. Kaplan–Meier method and log-rank test were applied. **(C)** Study design. *FVB/N* mice were hydrodynamically injected with sgPTEN/c-MET/SB. At six weeks after injection, one group of mice (N=5) was sacrificed, and liver tissues were harvested as the pre-treatment. Other mice were randomly assigned to the vehicle (N=5) or TVB3664 (N=5) treated groups. Mice were treated for three weeks and then sacrificed. **(D)** Liver weight in the three groups. **(E)** Representative images of H&E, PTEN, Ki67, and Oil-Red-O (ORO) stainings. Scale bars: 200μm for H&E, 100μm for PTEN, Ki67 (main images,) and Oil-Red-O. T: Tumor areas.**(F, G)** Comparisons of the percentages of PTEN negative area (F) and Ki67 positive cells (G) in the three groups. **(H)** Comparison of hepatic triglyceride (Trig.) levels in the sgPTEN/c-MET tumors (T) and

surrounding liver tissues (SL) in the vehicle and TVB3664 groups. (B) Log-rank (Mantel-Cox) test; (D, F, G) Mean ± SD; One-way ANOVA test; (H) Mean ± SD; Mann-Whitney test. **, $P<0.01$; ****, $P<0.0001$; NS, no significance.

A

Cell line	MHCC97H	HLE	SNU449
TVB3664 IC50 (μM)	39.23	23.52	43.16
Cabozantinib IC50 (μM)	7.19	15.24	35.30

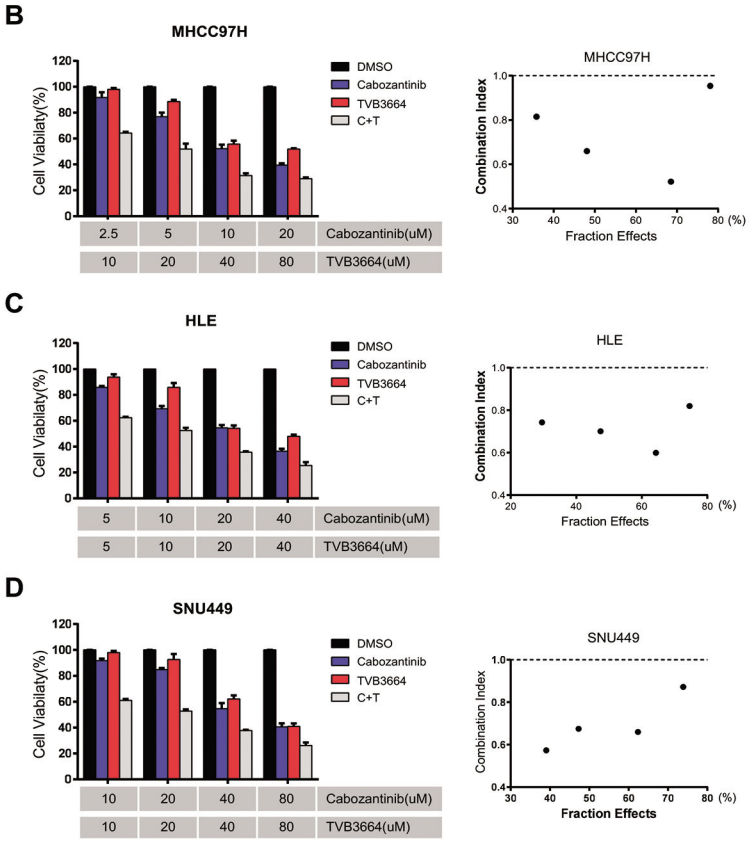

Fig. 3. Synergistic growth inhibitory effects of TVB3664 and cabozantinib in human HCC cell lines.

(A) IC50 values of cabozantinib and TVB3664 in the human HCC cell lines (MHCC97H, HLE, and SNU449). **(B-D)** Cell viability and combinational indexes in the DMSO, TVB3664, cabozantinib, and combinational treated groups with different concentrations as indicated in MHCC97H (B), HLE (C), and SNU449 (D) human HCC cells.

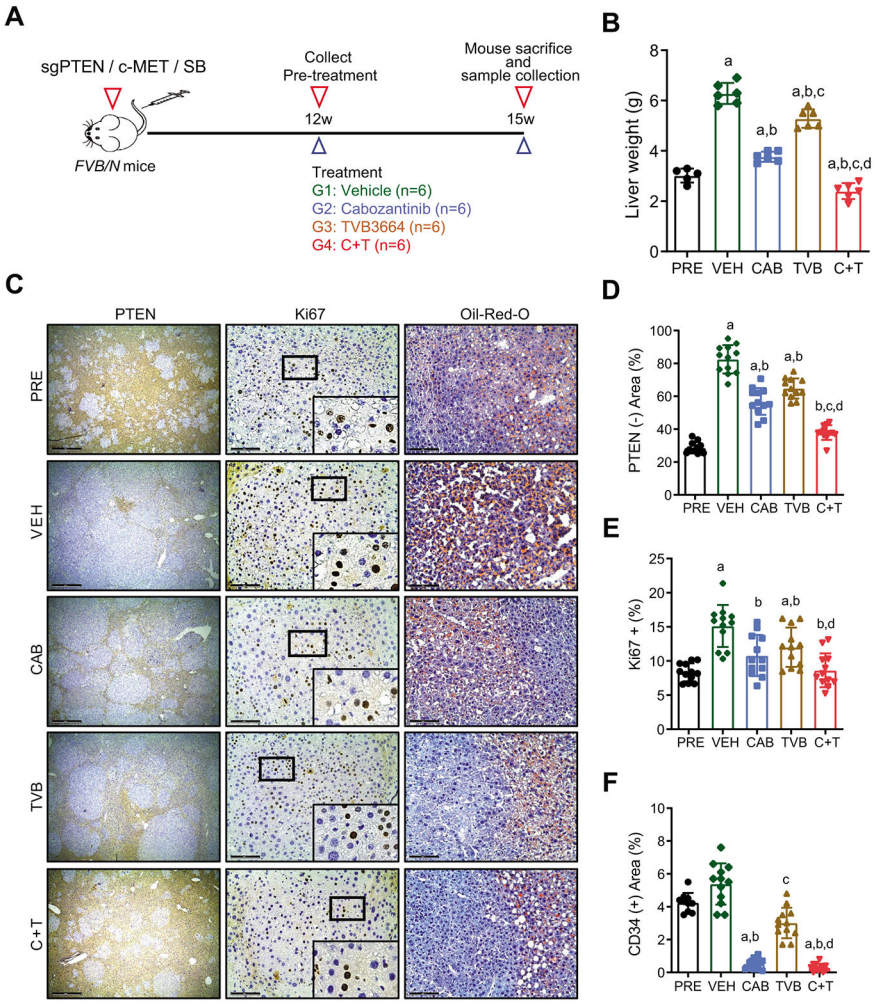

Fig. 4. TVB3664 combined with cabozantinib leads to the regression sgPTEN/c-MET mouse HCCs.

(A) Study design. *FVB/N* mice were hydrodynamically injected with sgPTEN/c-MET/SB. Twelve weeks after injection, one group of mice (N=5) was sacrificed, and liver tissues were harvested as the pre-treatment. Other mice were randomly assigned into the vehicle (VEH), Cabozantinib (CAB), TVB3664 (TVB), or Cabozantinib and TVB3664 combinational (C+T) treated groups. Mice were treated for three weeks and then sacrificed (fifteen weeks after injection). (B) Liver weight in the five groups. (C) Representative images of PTEN, Ki67, and Oil-Red-O stainings. (D-F) Comparison of PTEN negative areas (D), Ki67 positive cells (E), and CD34 positive areas (F) percentages in the five groups. Scale bars: 500μm for PTEN, 100μm for Ki67 (main images), and Oil-Red-O. (B, D, E, F) Mean ± SD; One-way ANOVA test. $P<0.05$ (a) vs. PRE; (b) vs. VEH; (c) vs. CAB; (d) vs. TVB.

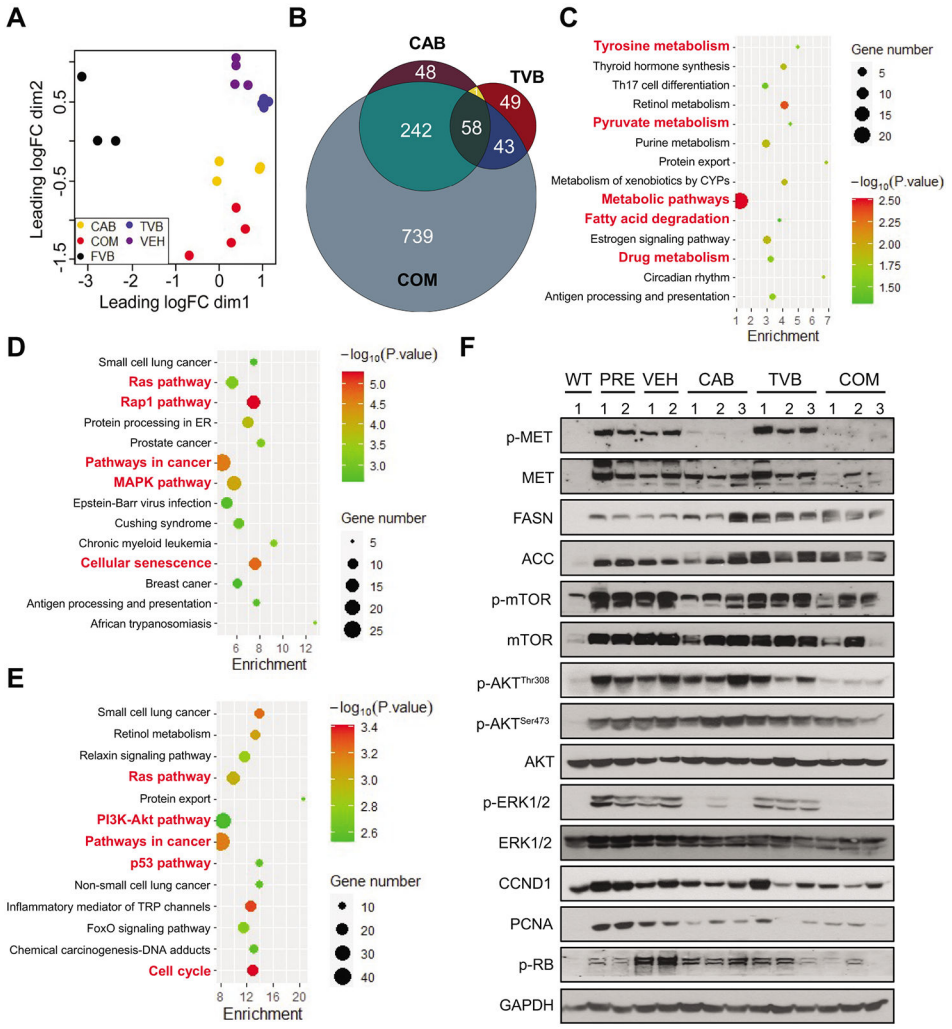

Fig. 5. Effects of TVB3664 and cabozantinib combinational treatment on the sgPTEN/c-MET mouse HCCs.

(A) Genetic dissimilarity among the samples in each group as demonstrated by multidimensional scaling (MDS). **(B)** Numbers of overlapped down-regulated genes in the Cabozantinib (CAB), TVB3664 (TVB), and Cabozantinib and TVB3664 (COM) treated samples as compared to the vehicle-treated samples. **(C-E)** KEGG analysis of down-regulated genes in the TVB3664 (C), Cabozantinib (D), and Cabozantinib and TVB3664 (E) combinational treated samples as compared to the vehicle-treated samples. **(F)** Analysis of the PI3K/AKT signaling pathway, major targets of cabozantinib, and cell cycle-related proteins. GAPDH was used as the loading control.

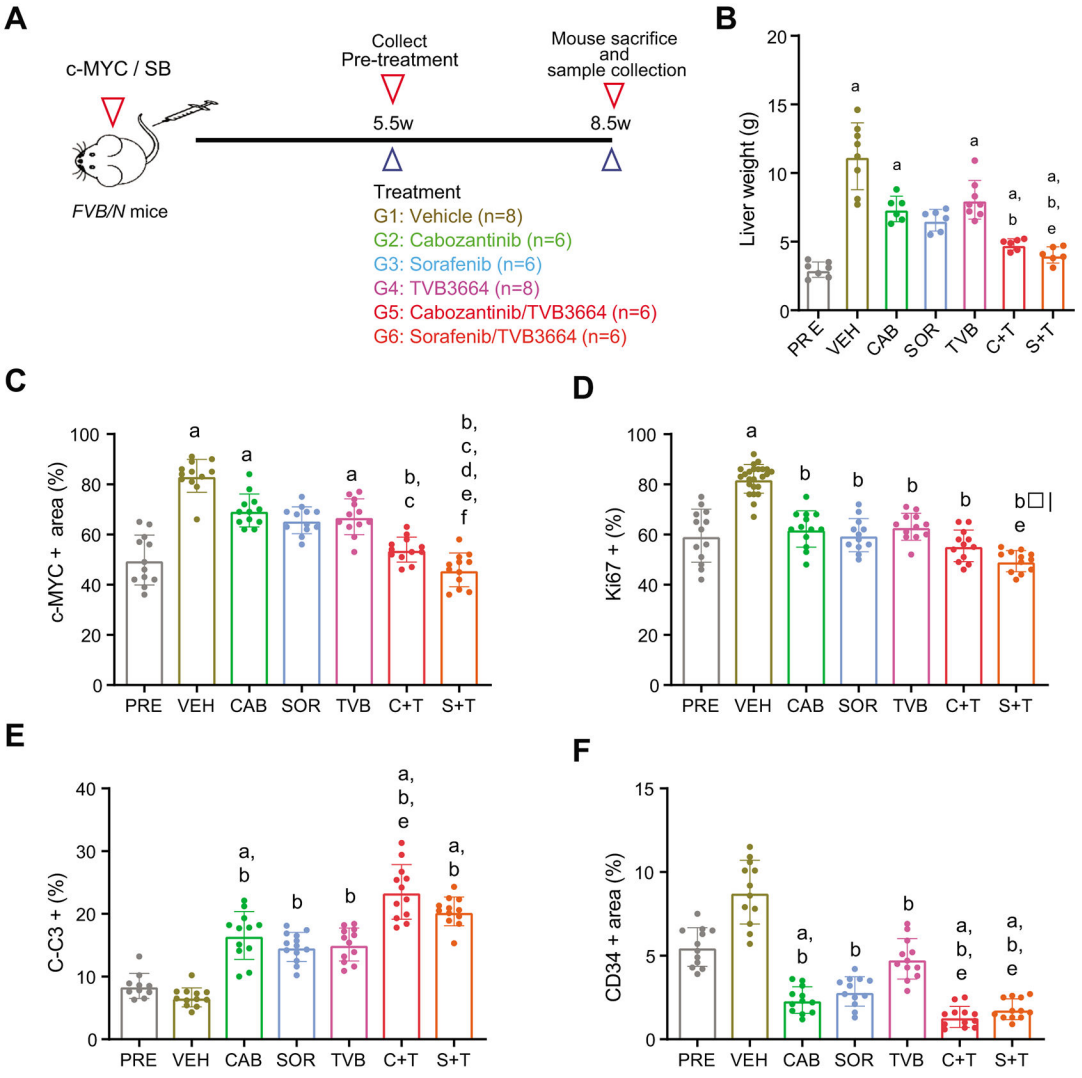

Fig. 6. TVB3664 acts synergistically with tyrosine kinase inhibitors to inhibit c-MYC hepatocarcinogenesis.

(A) Study design. *FVB/N* mice were hydrodynamically injected with c-MYC/SB. At 5.5 weeks after injection, one group of mice (N=7) was sacrificed, and liver tissues were harvested as the pre-treatment. Other mice were randomly assigned to the vehicle (VEH), cabozantinib (CAB), sorafenib (SOR), TVB3664 (TVB), or cabozantinib/TVB3664 (C+T) and sorafenib/TVB3664 combinational (S+T) treated groups. Mice were treated for three weeks and then were sacrificed. **(B)** Liver weight in the seven groups at the end of observation. **(C-F)** Comparison of percentages of c-MYC positive areas (C), Ki67 positive cells (D), cleaved caspase-3 (C-C3; E) positive cells, and CD34 positive areas (F) among the seven groups. (B, C, D, E, F) Mean ± SD; One-way ANOVA test. $P<0.05$ (a) vs. PRE; (b) vs. VEH; (c) vs. CAB; (d) vs. SOR; (e) vs. TVB; (f) vs. C+T.

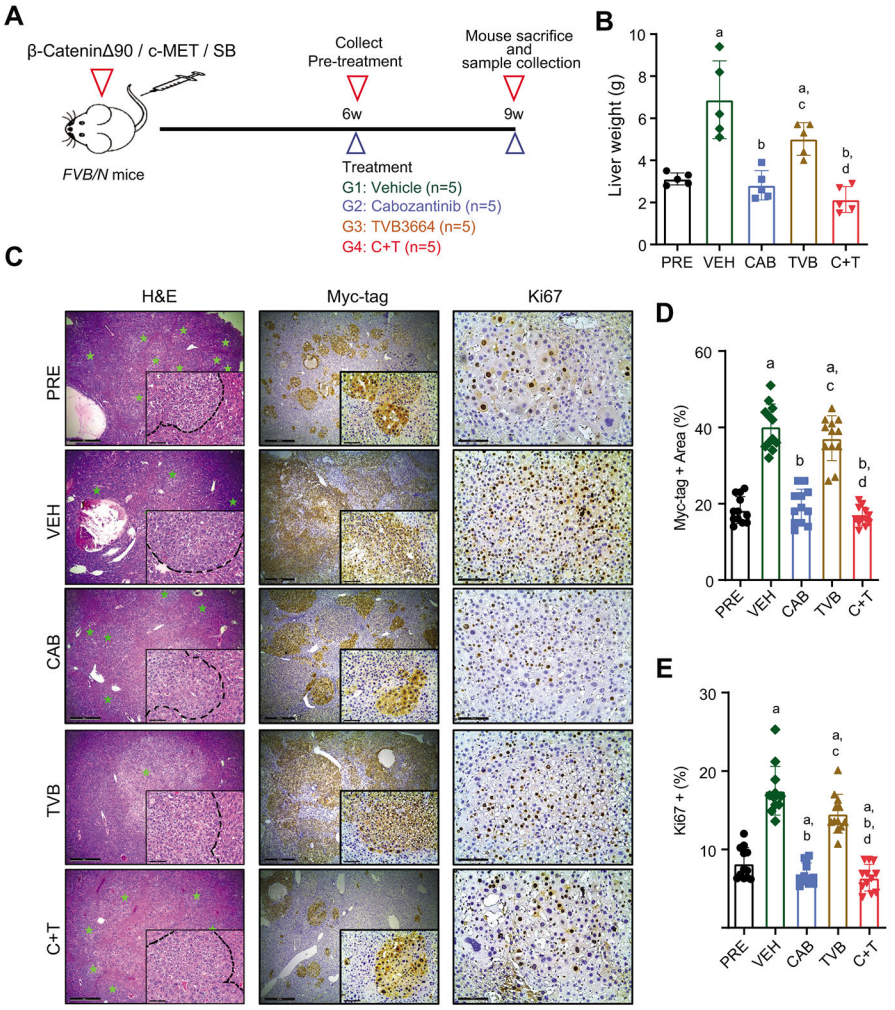

Fig. 7. TVB3664 marginally improves the anti-tumor activity of cabozantinib in the β-CateninΔ90/c-MET mouse HCCs.

(A) Study design. *FVB/N* mice were hydrodynamically injected with β-CateninΔ90/c-MET/SB. At six weeks after injection, one group of mice (N=5) was sacrificed, and liver tissues were harvested as the pre-treatment. Other mice were randomly assigned into the vehicle (VEH), Cabozantinib (CAB), TVB3664 (TVB), or Cabozantinib and TVB3664 combinational (C+T) treated groups. Mice were treated for three weeks and then were sacrificed. **(B)** Liver weight in the five groups. **(C)** Representative images of H&E, Myc-tag, and Ki67 stainings. Green asterisks inside the H&E images indicate tumor nodules. Scale bars: 500μm for H&E and Myc-tag (main images); 100μm for Ki67 and Myc-tag (insets). **(D, E)** Comparison of percentages of Myc-tag positive areas (D) and Ki67 positive cells (E) in the five groups. (B, D, E) Mean ± SD; One-way ANOVA test. P<0.05 (a) vs. PRE; (b) vs. VEH; (c) vs. CAB; (d) vs. TVB.